Journal of Physics: Conference Series

**PAPER** • **OPEN ACCESS**

# Resonant Activation of Resistance Switching in Memristors Based on YSZ Films with Au Nanoparticles

# Resonant Activation of Resistance Switching in Memristors Based on YSZ Films with Au Nanoparticles

**M A Ryabova[1,3], D O Filatov[1], M E Shenina[1], M N Koryazhkina[1], I N Antonov[2], V N Baranova[1,3] and O N Gorshkov[1]**

[1] Research and Education Center “Physics of the Solid State Nanostructures”, Lobachevsky State University of Nizhny Novgorod, 23 Gagarin Pr., Nizhny Novgorod, 603 022, Russian Federation
[2] Physical-Technical Research Institute, Lobachevsky State University of Nizhny Novgorod, 23 Gagarin Pr., Nizhnii Novgorod, 603 022, Russian Federation
[3] Department of Physics, Lobachevsky State University of Nizhny Novgorod, 23 Gagarin Pr., Nizhny Novgorod, 603 022, Russian Federation

Email: rmargo01@mail.ru

**Abstract.** The resonant activation of resistance switching (RS) of a memristor based on an yttria stabilized zirconia (YSZ) film with embedded Au nanoparticles (NPs) was investigated. The switching was made by triangular pulses with high frequency (HF) sinusoid added. A non-monotonous dependence a ratio of the electric current through the memristor in the low resistive state to the current in the high resistive one on the HF sinusoid frequency was found. The effect was explained by a finite electron tunneling time between the Pt electrode and Au NPs. This conclusion was supported by measuring a dependence of HF memristor capacitance on the probing signal frequency.

## 1. Introduction

In the past two decades, a phenomenon of resistance switching (RS) attracted an increased attention of researchers [1]. This phenomenon consists in a bistable (or in a multistable) non-volatile change of the resistive state of a thin-film capacitor when an appropriate voltage pulse is applied to this one [2]. The microelectronic devices utilizing the RS phenomenon were named “memory resistors” or *memristors* [3]. To date, the mechanism of RS based on so-called filamentary RS concept is a commonly accepted one [4]. This mechanism involves forming a conducting filament in the electric field inside the insulator until the filament shortcuts the capacitor plates. This way, the memristor is set to a low resistive state (LRS). One can reset the memristor back into the high resistive state (HRS) through a destruction of the filament in the reverse electric field. The filament may be restored again via the application of a voltage pulse of the opposite polarity. The mechanism of RS described here is usually referred to as the *bipolar* RS. In the memristors based on the transition metal oxides, the filaments are usually composed of oxygen vacancies ($V_O$s).

Currently, the memristors are considered to be promising for a wide range of applications, for example, in non-volatile resistive random access memory (RRAM) [5], in the novel computer architectures (including computing in the memory) [6], in the neuromorphic electronic circuits [7], etc. On the other hand, the application of the memristors is very limited at present because of an insufficient stability of the memristor parameters. This instability originates from an intrinsic stochasticity of the RS phenomenon [8].

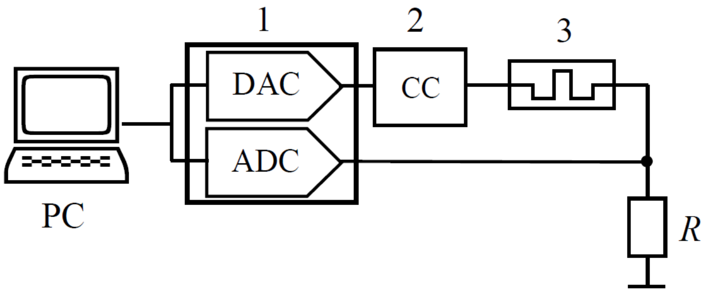


**Figure 1.** Scheme of the experiment. *1* –DAC/ADC module, *2* – current compliance unit, *3* – investigated memristor, *R* – resistor.

Earlier, we studied the prototype memristors based on YSZ films and bi-layered YSZ/$Ta_2O_5$ stacks [9, 10]. We found that an addition of a high frequency (HF) sinusoid to the triangular pulses improves the performance of the memristors. Similar results were obtained in the studies of RS in the YSZ films and in the YSZ/$Ta_2O_5$ stacks by Conducting Atomic Force Microscopy (CAFM) [11, 12]. In these investigations, a contact of the CAFM probe tip to the insulator films (or to the stacks) on the conductive substrates composed a nanometer-scale virtual memristive device [13]. The effect was related to a resonant activation of the electromigration (drift and/or diffusion) of the $O^{2-}$ ions through the $V_O$s due to the alternating electric field [14].

The present paper is devoted to an investigation of the resonant activation phenomenon in a memristive device based on a Ta/YSZ/Pt stack with Au nanoparticles (NPs) embedded near the Pt electrode. The NPs were expected to improve the RS performance further acting as the electric field concentrators [15].

## 2. Experiment

The nanocomposite YSZ:NP-Au film was fabricated by the deposition of a 3-layer stack including a 2-nm thick Au film sandwiched between two YSZ (≈12% mol. $Y_2O_3$) layers of 1 and 19 nm thick, respectively. The heavily doped *n*-type silicon substrate with a pre-deposited Pt sublayer of 10 nm in thickness was used. The stack was annealed at 450 °C during 2 min. Earlier, we found that the Au film transforms into a planar array of spherical Au NPs with the diameters ranging from 2 to 3 nm after annealing in the regime specified above [16]. Afterwards, the round Au top electrodes of 0.5 mm in diameter and 40 nm in thickness with 40-nm thick Ta sublayers were deposited through a shadow mask. The metal and YSZ films were made by the direct current and radio-frequency magnetron deposition at the substrate temperatures 200 and 300 °C, respectively, with Torr International® vacuum setup for the deposition of thin films.

The preliminary electrical characterization of the prototype memristors was performed at 300 K by acquiring several current-voltage ($I$−$V$) curves with an Agilent® B1500A analyzer of semiconductor devices. The electrical contact to the top electrode of the prototype memristor was made by an EverBeing® EB-6 microprobe station. Also, the zero-bias frequency dependencies of the memristor capacitance $C$, HF conductivity $G$, and dielectric loss angle tangent tgδ were measured in the HRS using the same instrument. The HF testing signal amplitude was 100 mV.

The RS was investigated at 300 K using the setup shown in figure 1. A digital-to-analog converter (DAC) of an USB-6361 DAC/ADC module (National Instruments®) operated under the control of a LabVIEW™ system was utilized as a computer-controlled voltage source. The DAC output rate was 2 MHz. The output voltage $V$ was supplied to the investigated memristor via a current compliance unit set to 500 μA. The memristor current response $I$ was taken from a load resistor $R$ = 100 Ω and directed to an analog-digital converter (ADC) of the DAC/ADC module. The sampling rate was 2 MHz.

The impact of the HF signal on the memristor performance was studied using the protocol (the dependence $V(t)$, $t$ being the time) shown in figure 2. The cyclic write/erase operations (switching back and forth) were made by the triangle voltage pulses with the magnitudes $V_{SET}$ = 1.5 V and $V_{RESET}$ = –1.4 V, respectively and durations $T_{SET}$ = $T_{RESET}$ = 1 s.

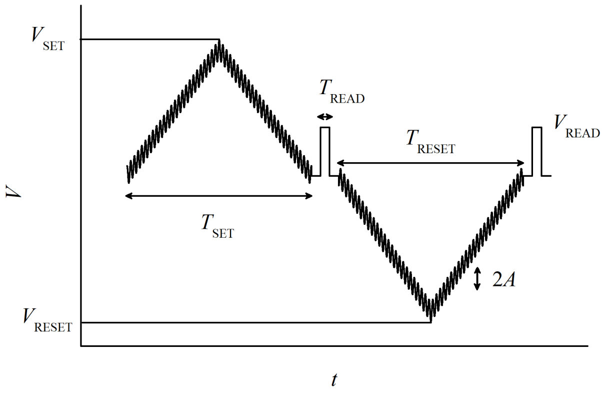


**Figure 2.** The protocol (the dependence $V(t)$, qualitatively) of measuring the impact of the HF signal on the RS performance.

The HF signal was added to the switching pulses. The characteristics of the HF signal were as follows: the amplitude $A$ = 100 mV; the frequency $f$ varied within the range from 10 Hz to 1 MHz The magnitudes of the electric current $I$ flowing via the memristor were recorded in the LRS ($I_{ON}$) as well as in the HRS ($I_{OFF}$) by applying the reading voltage pulses with the amplitudes $V_{READ}$ = 0.5 V and durations $T_{READ}$ = 50 ms and averaged over 10 000 readouts per each read operation. Total 100 write/read/erase/read cycles were performed for each value of $f$.

## 3. Results and discussion

Several $I$–$V$ curves of the prototype memristor fabricated from the YSZ film with Au NPs are shown in figure 3. The $I$–$V$ curves were measured without the supply of the HF sinusoidal signal. A hysteresis has been observed, which points to the bipolar RS.

Figure 4a shows a frequency dependence of the mean $I_{ON}/I_{OFF}$ ratio on for the memristor based on the YSZ:NP-Au film (the values of the $I_{ON}/I_{OFF}$ ratio were averaged over 100 switching cycles). This dependence manifested a pronounced peak in the range of $f$ from 100 kHz to 1 MHz. This peak can be explained as follows. Figure 4b shows the frequency dependencies of the zero-bias capacitance $C$, the HF conductance loss $G/\omega$ (the HF conductivity $G$ normalized to the circular frequency $\omega = 2\pi f$), and the dielectric loss angle tangent tg$\delta$ for the same memristor. All these dependencies were measured in the HRS. The values of $C$ decrease with increasing $f$ and begin to decrease faster at $f \sim 1$ MHz. This can be explained by tunneling of electrons from the bottom Pt electrode into the Au NPs separated by a thin (tunnel transparent) YSZ layer and back [17] (see the calculated band picture of the Ta/YSZ:NP-Au/Pt stack in figure 5). The electron-tunneling rate between the Au NP and the Pt electrode can be estimated as follows. The tunneling transparency $T$ of the potential barrier between an Au NP in YSZ and the Pt electrode can be evaluated from a semiclassical expression for the tunnel transparency of a trapezoidal potential barrier:

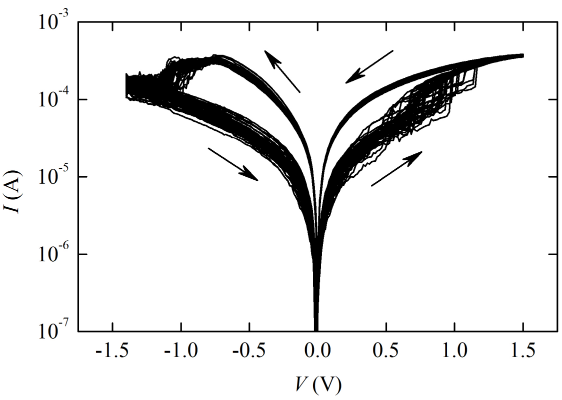


**Figure 3.** The $I$−$V$ curves of the prototype memristor fabricated from the YSZ:NP-Au film measured without the HF signal.

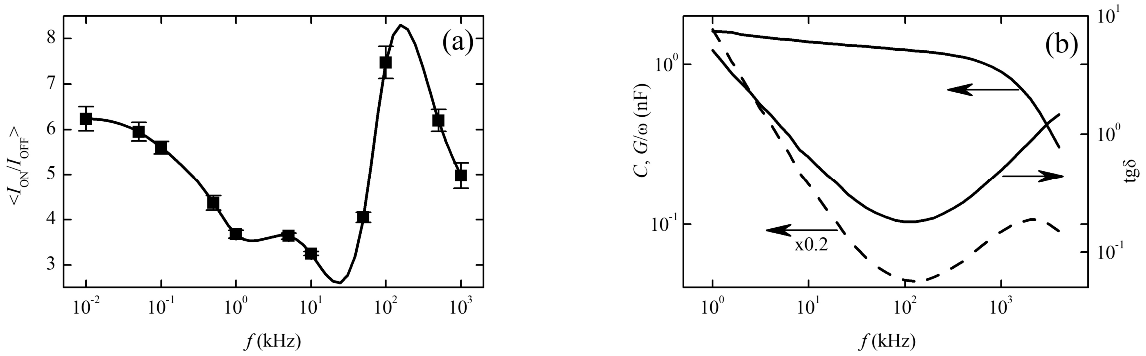


**Figure 4.** (a) Dependence of the mean $I_{ON}/I_{OFF}$ ratio on HF sinusoid frequency $f$ for the memristor fabricated from the YSZ:NP-Au film; (b) the frequency dependencies of the zero-bias capacitance $C$ (solid line), the HF conductance loss $G/\omega$ (dashed line), and the dielectric loss angle tangent tgδ for the same device.

$$T \sim \exp\left(-\frac{2l}{\hbar}\sqrt{2mU}\right), \tag{1}$$

where $U$ is the mean potential barrier height, $m$ is the effective electron mass in YSZ, $\hbar$ is the reduced Planck constant, and $l$ is the potential barrier width (the spacing between the Au NP and the Pt electrode).

Let us consider the tunnel escape of electrons with Fermi energy in the Au NP $E_F$ to the Pt electrode. In the steady state, its rate should be equal to the one of the electron tunneling from the Pt electrode back to the Au NP. One has $U = (E_{Pt} + E_{Au})/2$, $E_{Pt}$ and $E_{Au}$ being the potential barrier heights (the energy spacings from the bottom of conduction band in YSZ to Fermi energy in Pt and in Au, respectively). One can estimate the mean escape time for an electron with the Fermi energy in the Au NP to the Pt electrode as $\tau_t \sim 2D/v_F T$, where $v_F$ is velocity of electrons with Fermi energy, $D$ is NP diameter. Taking $v_F = 1.4\ 10^6$ m/s for Au [18], $E_{Au} = 2.5$ eV, $E_{Pt} = 3.0$ eV (see the calculated band picture of the Ta/YSZ:NP-Au/Pt stack presented in figure 5), $m = 0.6m_0$ [19] ($m_0$ being the free electron mass), one gets for $D = 2$ nm $\tau_t \approx 2\cdot 10^{-6}$ s, that corresponds to the frequency $f_t = 1/\tau_t \sim 500$ kHz. This value matches well to the HF peak position in figure 4a. At $f < f_t$, the electrons can tunnel between the Au NPs and the Pt electrode with the variation of HF component of the voltage $V(t)$ applied. Every time the next electron enters the Au NP, its potential increases by the Coulomb potential $\Delta V_C \sim e/C_p$. Here $e$ is the electron charge, $C_p$ is partial capacitance between the NP and the Pt electrode. The latter can be estimated using an approximate formula [20]:

$$C_p \sim \pi\varepsilon\varepsilon_0 D\left(2 + \frac{D}{2l}\right), \tag{2}$$

where $\varepsilon_0$ is the electric constant and $\varepsilon$ is the relative dielectric permittivity of YSZ. Taking $\varepsilon = 20$ [19], one gets $\Delta V \approx 50$ mV for $l = 1$ nm and $D = 2$ nm. Hence, at $A = 100$ mV, such a NP can accommodate 2 extra electrons until Coulomb blockade of tunneling takes place. Accordingly, the dielectric field strength at the Au NP surface $F_c$ increases and decreases synchronously with the HF sinusoidal signal due to the tunnel injection of electrons from the Pt electrode into the Au NP and their extraction back to the Pt electrode. As it has been shown in [21], charging of such a small NP in the same system by even a single electron results in an essential variation of $F_c$ (in $\sim 10^6$ V/cm), which is sufficient to affect the RS. However, at $f > f_t$ the electron tunneling cannot follow the external electric field anymore. This is manifested as the decrease in $C$ in figure 4b and, correspondingly, as the decrease in the mean $I_{ON}/I_{OFF}$ ratio in figure 4a.

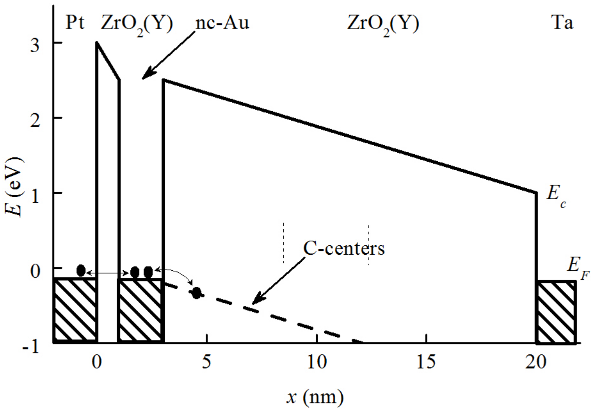


**Figure 5.** Calculated band picture (300 K) of the Ta/YSZ:NP-Au/Pt memristor. The values of electron affinity for YSZ and of workfuncions for the metals were taken from [19] and [23], respectively.

A decrease in the mean $I_{ON}/I_{OFF}$ ratio in the range of $f$ from ~100 Hz to ~100 kHz (figure 4a) can be explained as follows. One can see the values of $G/\omega$ and of tgδ decrease in this frequency range (figure 4b). It points to some HF dielectric loss having a resonant character (the maximum loss at $f \sim 100$ kHz). Earlier, a nonlinear capacitance (with some hysteresis) of the prototype memristors based on the YSZ:NP-Au nanocomposite films was revealed by HF $C$–$V$ spectroscopy [22]. The nonlinear capacitance was explained by trapping of electrons by the Au NPs. Also, some thermally activated process was observed with the activation energy $E_a \approx 0.3$ eV, but its nature remained unclear. It should be stressed here that no such phenomena were observed for the memristors made on the base of pure YSZ films without NPs.

In our opinion, the above activation process may be explained by the thermally activated excitation of the electrons from the deep levels (the C-centers) with ionization energy ≈ 2.6 eV (related to the $V_O$s in YSZ [24]) into Au NPs (see figure 5). The enhanced dielectric loss observed in the present work can also be attributed to this process. Note that such a process includes tunneling of electrons between the NPs and the C-centers in YSZ, located somewhere near the NPs. In this scope, the large width of the drop of the $G/\omega(f)$ and tgδ($f$) dependencies can be attributed to a random distribution of spacings between the traps and the NPs, in turn, originating from a random distribution of the $V_O$s in the YSZ lattice.

When $f > 1$ MHz, the values of $G/\omega$ and $C$ decrease with increasing $f$ (see figure 4b). Again, it can be attributed to switching off the tunneling between the Au NPs and the Pt electrode.

Finally, a small increase in the mean $I_{ON}/I_{OFF}$ ratio in the range of $f$ from ~ 1 kHz to ~ 10 kHz can be explained by resonant activation of electromigration of the $O^{2-}$ ions through $V_O$s [9-12, 14].

## Conclusion

In the present work, the RS parameters of memristive device made on the base of Ta/YSZ:NP-Au/Pt thin film stack have been studied using triangular voltage pulses and superimposed HF sinusoid as the driving voltage. A non-monotonous dependence of the mean $I_{ON}/I_{OFF}$ ratio was observed. This non-monotonous dependence was explained by the tunneling of electrons between Au NPs and the bottom Pt electrode. This conclusion was justified on the base of the frequency dependence of the memristor capacitance. Also, non-monotonous frequency dependencies of the HF conductance loss and of the dielectric loss angle tangent were observed. Such a behavior was ascribed to the thermally activated electron excitation from the C-centers in YSZ into the Au NPs. This effect can explain qualitatively the decrease in the $I_{ON}/I_{OFF}$ ratio in the frequency range from 100 Hz to 100 kHz. However, to understand this effect in more details, further investigations are necessary.

## Acknowledgements

The authors gratefully acknowledge the financial support from RFFI (Project # 18-42-520059r_a). The experiments were done using the instrumentation of Research and Education Center “Physics of the Solid State Nanostructures”, Lobachevsky State University of Nizhny Novgorod.

## References

[1] Shi T, Wang R, Wu Z, Sun Y, An J and Liu Q 2021 *Smart Materials* **2** 2000109
[2] Celano U 2016 *Metrology and Physical Mechanisms in New Generation Ionic Devices* (Berlin-Heidelberg: Springer)
[3] Hazra A 2012 *Resistive Random Access Memory: The New Generation High Speed Switching Non-Volatile Memory Device* (LAP LAMBERT Academic)
[4] Rupp J, Ielmini D and Valov I 2021 *Resistive Switching: Oxide Materials, Mechanisms, Devices and Operations* (Berlin-Heidelberg: Springer)
[5] Yu S 2016 *Resistive Random Access Memory (RRAM)* (Williston: Morgan & Claypool)
[6] Chua L O 2022 *Memristor Computing Systems* (Berlin-Heidelberg: Springer)
[7] Li Y, Wang Z, Midya R, Xia Q and Yang J 2018 *Journal of Physics D: Applied Physics* **51** 503002
[8] Alonso F J, Maldonado D, Aguilera A M and Roldán J B 2021 *Chaos, Solitons & Fractals* **143** 110461
[9] Filatov D O, Antonov D A, Antonov I N *et al.* 2020 *Physics of Solid State* **62** 64
[10] Baranova V N, Filatov D O, Antonov D A *et al.* 2020 *Semiconductors* **54** 1830
[11] Filatov D O, Koriazhkina M N, Antonov D A *et al.* 2019 *Technical Physics* **89** 1669
[12] Filatov D O, Koriazhkina M N, Antonov D A *et al.* 2019 *IOP Conference Series: Materials Science and Engineering* **699** 012012
[13] Kim Y-M, Lee J, Jeon D-J, Oh S-E and Yeo J-S 2021 *Applied Microscopy* **51** 7
[14] Ryabova M A, Filatov D O, Koriazhkina M N *et al.* 2021 *Journal of Physics: Conference Series* **1851** 012003
[15] Chen Z *et al.* 2020 Patent CN211743191U
[16] Gorshkov O N, Antonov I N, Filatov D O *et al.* 2017 *Advances in Materials Science and Engineering* 1759469
[17] Zeller H R and Giaver I 1969 *Physical Review* **181** 789
[18] Kroemer H and Kittel C 1980 *Thermal Physics* (W. H. Freeman Co.)
[19] Shnikov V, Gritsenko D V, Petrenko I P *et al.* 2006 *Journal of Experimental and Theoretical Physics* **102** 799
[20] Antonov D A, Filatov D O, Zenkevich A V *et al.* 2007 *Izvestiya Akademii Nauk, Seria Fizichekaya* **71** 61
[21] Novikov A S, Filatov D O, Shenina M E e*t al*. 2021 *Journal of Physics D: Applied Physics* **54** 485303
[22] Tikhov S V, Gorshkov O N, Pavlov D A *et al.* 2014 *Technical Physics Letters* **40** 369
[23] *Landolt-Borstein's Zahlenwerte und Funktionen aus Physik, Chemie, Astrunumie, Geophysik, Thechnik* 1960 (Springer: Berlin)
[24] Nakajima H and Mori T 2006 *Journal of Alloys and Compounds* **408–412** 728